



## ORIGINAL ARTICLE

# Prominin-1 deletion results in spermatogenic impairment, sperm morphological defects, and infertility in mice

Haruka Matsukuma<sup>1</sup>  | Yuka Kobayashi<sup>2</sup> | Shintaro Oka<sup>1</sup> | Fumiaki Higashijima<sup>2</sup> | Kazuhiro Kimura<sup>2</sup> | Erika Yoshihara<sup>3</sup> | Noriaki Sasai<sup>3</sup> | Koji Shiraishi<sup>1</sup> 

<sup>1</sup>Department of Urology, School of Medicine, Yamaguchi University, Ube, Japan

<sup>2</sup>Department of Ophthalmology, School of Medicine, Yamaguchi University, Ube, Japan

<sup>3</sup>Developmental Biomedical Science, Division of Biological Sciences, Nara Institute of Science and Technology Ikoma, Nara, Japan

## Correspondence

Koji Shiraishi, Department of Urology, Yamaguchi University School of Medicine, Minami-Kogushi 1-1-1, Ube 755-8505, Japan.  
Email: [shirak@yamaguchi-u.ac.jp](mailto:shirak@yamaguchi-u.ac.jp)

## Funding information

Japan Society for the Promotion of Science, Grant/Award Number: 22K09475

## Abstract

**Purpose:** Spermatogenesis is a complex process orchestrated by several essential genes. *Prominin-1* (*Prom1*/PROM1) is a gene that is expressed in the testis but with a poorly understood role in spermatogenesis.

**Methods:** We used *Prom1* knockout (*Prom1* KO) mice to assess the role of *Prom1* in spermatogenesis. To this end, we performed immunohistochemistry, immunofluorescence, western blotting,  $\beta$ -galactosidase staining, and apoptosis assay. Additionally, we analyzed the morphology of sperm and assessed litter sizes.

**Results:** We observed that PROM1 is localized to the dividing spermatocytes in seminiferous epithelial cells, sperm, and columnar epithelium in the epididymis. In the *Prom1* KO testis, an aberrant increase in apoptotic cells and a decrease in proliferating seminiferous epithelial cells were observed. Cellular FLICE-like inhibitory protein (c-FLIP) and extracellular signal-regulated kinase 1/2 (ERK1/2) expression were also significantly decreased in *Prom1* KO testis. In addition, a significantly increased number of epididymal spermatozoa with abnormal morphology and less motility was found in *Prom1* KO mice.

**Conclusions:** PROM1 maintains spermatogenic cell proliferation and survival via c-FLIP expression in the testis. It is also involved in sperm motility and fertilization potential. The mechanism underlying the effect of *Prom1* on sperm morphology and motility remains to be identified.

## KEYWORDS

flagellum function, *Prom1* KO mice, *Prominin-1*, sperm morphology, spermatogenesis

## 1 | INTRODUCTION

Male fertility is maintained through the continuous production of germ cells, which is the only cell type that divides into haploid cells and carries genetic information across generations. Male germ cells differentiate into spermatozoa via spermatogenesis, a complex process that involves a series of mitosis, two stages of meiosis, and a post-meiotic differentiation.<sup>1</sup>

*Prominin-1* (*Prom1*; also known as RP41, CD133, AX133, and STGD4; NCBI gene ID 8842) encodes a pentaspan transmembrane glycoprotein with a molecular weight of approximately 120kDa.<sup>2</sup> It was initially identified in primitive hematopoietic and neural epithelial cells<sup>3,4</sup> and is involved in the regulation of cell morphology and migration.<sup>5,6</sup> In epithelial cells, PROM1 is concentrated in microvilli and is involved in plasma membrane protrusion.<sup>4</sup> Other reports suggest that PROM1 induces cell membrane extensions that are involved in

This is an open access article under the terms of the [Creative Commons Attribution-NonCommercial-NoDerivs](https://creativecommons.org/licenses/by-nc-nd/4.0/) License, which permits use and distribution in any medium, provided the original work is properly cited, the use is non-commercial and no modifications or adaptations are made.

© 2023 The Authors. *Reproductive Medicine and Biology* published by John Wiley & Sons Australia, Ltd on behalf of Japan Society for Reproductive Medicine.

cell migration.<sup>5</sup> *Prom1* is not only expressed in normal stem cells but also cancer stem cells (CSC) of high-grade breast tumors.<sup>7</sup> Recently, *Prom1* was found to be expressed in most CSCs emerging in the brain,<sup>8</sup> bone,<sup>9</sup> skin,<sup>10</sup> lung,<sup>11</sup> liver,<sup>12</sup> colon,<sup>13</sup> pancreas,<sup>14</sup> kidney,<sup>15</sup> bladder,<sup>16</sup> prostate,<sup>17</sup> and ovary.<sup>18</sup> In tumors, PROM1 upregulates the expression of cellular FLICE-like inhibitory protein (c-FLIP),<sup>19</sup> which activates the extracellular signal-regulated kinase 1/2 (ERK 1/2), c-Jun N-terminal kinase, and Wnt and protein kinase B (Akt) pathways, leading to increased cell proliferation and survival.<sup>20–23</sup> In addition, c-FLIP suppresses activation of pro-caspase 8,<sup>24</sup> which in turn inhibits cell apoptosis.

Several studies have reported that PROM1 is also localized in the testis.<sup>25,26</sup> Therefore, the function of PROM1 in cancer cells may be conserved in spermatogenesis, with regard to regulation of cell proliferation and differentiation. Consistently, *Prom1* expression levels in patients with non-obstructive azoospermia (NOA) were lower than those in healthy males and patients with obstructive azoospermia.<sup>27</sup> These pathological observations suggest an important role of *Prom1* in spermatogenesis and fertility. However, mechanistic analyses investigating the role of PROM1 in spermatogenesis have not been conducted.

In the present study, we address this point by using *Prom1* knockout (KO) mice and have studied the intracellular localization of PROM1 in the testis and analyzed sperm morphology, histology of sperm epithelial cell division, and expression of several relevant signaling molecules to examine the functioning of *Prom1* in spermatogenesis.

## 2 | MATERIALS AND METHODS

### 2.1 | Animals

All animal experiments were approved by the Committees for Ethics on Animal Experiments of Yamaguchi University School of Medicine (J16021) and Nara Institute of Science and Technology and were conducted in accordance with international and national guidelines.

The *Prom1* KO mouse line was established previously<sup>28,29</sup> (CDB0623K: <http://www2.clst.riken.jp/arg/methods.html>). Mutant mice harboring the *LacZ* gene at the *Prom1* locus were maintained in the C57BL/6 background, with a 12-h day/night cycle and ad libitum access to food and water. Litter size was evaluated by mating *Prom1* KO male mice with heterogeneous female mice for 6 months, and the total number of pups was recorded.

### 2.2 | Genotyping

Tail snips of 4-week-old mice were cut and immersed in 50mM NaOH at 90°C for 10 min. Ten microliters of 1M Tris-HCL (pH 7.6) was added to each sample and incubated for 4 h at 24°C. The samples were centrifuged at 10000g for 10 min at 4°C to pellet the DNA. Polymerase chain reaction (PCR) was performed using a

commercially available kit (DTM-101, TOYOBO) following the manufacturer's protocol. The primers used are listed in Figure S1.

### 2.3 | Breeding potential of *Prom1*-mutant female mice

Breeding pairs between female and male mice of various genotypes were set up, with the number of days between the start of mating and birth of pups being recorded.

### 2.4 | Mating and assessment of breeding potential

To assess the breeding potential of male mice, with genotypes of *Prom1*<sup>+/+</sup>, *Prom1*<sup>+/-</sup>, and *Prom1*<sup>-/-</sup> were housed with two female *Prom1*<sup>+/-</sup> mice aged 8–30 weeks. The litter number in each cage was recorded every month; at the end of the fertility test, testes were collected for histological analyses (Figure 3A,B). The littermates found in each cage were used for subsequent analyses.

To investigate fertility by genotype in female mice, those with various genotypes were bred with male mice of different genotypes, all aged 8 weeks (Figure 3), with the number of days taken to give birth being examined (Figure 3C).

### 2.5 | $\beta$ -Galactosidase staining

Testis and epididymis were fixed with 4% paraformaldehyde (PFA) for 2 h and incubated in 15% sucrose overnight. The samples were embedded in an optimal cutting temperature (O.C.T) compound (Sakura Finetek). The sections were prepared using a TissuePolar cryostat (Sakura Finetek). Sectional samples were rinsed in 1× phosphate-buffered saline (PBS) (Wako Pure Chemical Industries, Ltd.) and stained with  $\beta$ -gal solution (5 mM K<sub>3</sub>[FeCN]<sub>6</sub>, 5 mM K<sub>2</sub>[FeCN]<sub>6</sub>, and 2 mM MgCl<sub>2</sub>) supplemented with X-Gal solution (Nacalai Tesque) at 37°C. After staining, the samples were rinsed and fixed in 4% PFA/1× PBS for 10 min, and mounted with mounting medium (Matsunami Glass Co.) and coverslips. Images were captured using Axioplan 2 (Carl Zeiss).

### 2.6 | Measurement of the number and motility of spermatozoa

Freshly dissected sections of the *cauda epididymis* were chopped and incubated in Toyoda, Yokoyama, Hoshi medium (LSI Medience Co.), at 24°C to release the spermatozoa. Sperm suspensions were loaded onto a MAKLER counting chamber (SEFI medical instruments). Spermatozoa were counted three times and classified as motile or immotile. Sperm morphologies were analyzed by pulling a smear with a centrifuged pellet at 6000g for 5 min and classified into four types according to the shape of the tail: normal, hairpin, half-hairpin, and absent. Hairpins

were classified as sperms with tails bent more than 180°, and half-hairpins were classified as those with tails bent 90°–180°. Absent refers to sperms with no tails. Three mice were analyzed for each genotype, with several images being taken at random for each, while spermatozoa were classified using the above criteria.

## 2.7 | Western blotting

Extracted organs were homogenized in sampling buffer (T-per Thermo Fisher Scientific) and were centrifuged for 5 min at 10000g, and the supernatant was collected. Proteins (10 µg) were separated using sodium dodecyl sulfate-polyacrylamide gel electrophoresis (SDS-PAGE) and transferred to polyvinylidene difluoride membranes (Bio-Rad Laboratories). The following primary antibodies were used: mouse anti-β-actin (RRID: AB\_10697039, #M177-3, 1:1000 dilution; MBL), rabbit anti-CD133 (RRID: AB\_2172859, #18470-1-AP, 1:1000 dilution; Proteintech), rabbit anti-phospho-histone H3 (RRID: AB\_310177, #06-570, 1:1000 dilution; Millipore), rabbit anti-FLIP (RRID: AB\_10013746, #8510, 1:1000 dilution; CST), rabbit anti-Phospho-p44/42 MAPK (pERK1/2) (RRID: AB\_331775, #4377, 1:1000 dilution; CST), and rabbit anti-ERK1 (RRID: AB\_631453, #sc-93, 1:200 dilution; Santa Cruz Biotechnology). The membranes were then washed with Tris-buffered saline (TBS) with 0.1% Tween 20 and incubated for 1 h at 24°C in a blocking solution (no. NYPBR01, TOYOCO) with horseradish peroxidase (HRP)-conjugated secondary antibodies. The following secondary antibodies were used: goat anti-mouse IgG (RRID: AB\_2755049, no. ab205719, 1:2500 dilution; Abcam) and goat anti-rabbit IgG (RRID: AB\_955447, no. ab6721, 1:2500 dilution; Abcam). Immunoreactive bands were developed using an enhanced chemiluminescent (ECL) kit (Cytiva) according to the manufacturer's protocol. Immunospecific bands were quantified using ImageJ software (ImageJ®, version 1.52a; National Institutes of Health). Densitometric values were normalized to those from β-actin.

## 2.8 | Histology, apoptosis assay, immunohistochemistry, and immunofluorescence

Testis samples were dissected and fixed with Bouin's fixative overnight for hematoxylin and eosin staining, apoptosis assays, and immunohistochemistry, and in PFA fixative for 24 h for immunofluorescence. The samples were then dehydrated and embedded in paraffin. Tissues were sectioned at 5 µm using a microtome and mounted on glass slides.

For hematoxylin staining, the sections were deparaffinized, rehydrated, and incubated in hematoxylin (Wako Pure Chemical Industries, Ltd.) for 1 min at 24°C and then rinsed in running water for 1 min.

To detect the apoptotic cells, a deoxynucleotidyl transferase-mediated dUTP nick end labeling (TUNEL) assay was performed. The

TUNEL staining was performed using a commercially available kit (no. 293-71501, Wako Pure Chemical Industries, Ltd.) following the manufacturer's protocol. Following deparaffinization and rehydration, the tissue samples on the glass slides were digested with proteinase solution at 37°C for 5 min. Samples were washed with PBS and treated with 100 µL TdT reaction solution for 10 min in a moist chamber at 37°C. Thereafter, the samples were washed with PBS, and intrinsic peroxidase activity was inhibited by treatment with 3% H<sub>2</sub>O<sub>2</sub> for 5 min at 24°C. The slides were then washed with PBS and covered with 100 µL POD-conjugated antibody solution for 10 min in a moist chamber at 37°C. Subsequently, the samples were washed again with PBS, and the slides were incubated with diaminobenzidine tetrahydrochloride (DAB) (#415171; NICHIREI Biosciences) for 10 min at 24°C and rinsed in running water. Finally, the slides were counterstained with hematoxylin for 1 min, dehydrated, and observed under a microscope (Keyence BZ-X800). TUNEL-positive cells in 100 seminiferous tubules were counted, and the ratio of TUNEL-positive cells per tubule was compared between the different genotype groups.

For immunohistochemistry, following deparaffinization and rehydration, endogenous peroxidase activity was blocked by incubation with methanol containing 3% (v/v) hydrogen peroxide for 10 min. For antigen retrieval, the slides were microwaved in citrate buffer (pH 6.0) (LSI Medience Co.) for 15 min and cooled for 1 h at 24°C. After blocking with 2% bovine serum (Sigma-Aldrich) in PBS for 30 min, the slides were incubated overnight at 4°C with primary antibodies in the blocking solution. The following primary antibodies were used: rabbit anti-PROM1 (RRID: AB\_1846238, HPA004922; Sigma-Aldrich) at 1:400 dilution. After washing with TBS, slides were incubated with HRP-conjugated secondary antibody (no. 414191, NICHIREI Biosciences) in the blocking solution for 30 min at 37°C. Slides were then incubated with DAB (no. 415171; NICHIREI Biosciences) and observed under a microscope (Keyence BZ-X800).

For immunofluorescence, tissue samples were processed using the same protocol as that used for immunohistochemistry until incubation with the primary antibody; rabbit anti-phospho-histone H3 (RRID: AB\_310177, #06-570; Millipore) at 1:400 dilution. Slides were then incubated for 30 min at 37°C in the blocking solution with Alexa Fluor 488 secondary antibodies (RRID: AB\_2630356, #ab150077; Abcam) at 1:1000 dilution. The slides were stained then with 4',6-diamidino-2-phenylindole (DAPI) for nuclear staining and mounted with an anti-fade reagent. Observations were made using a microscope (Keyence BZ-X800).

## 2.9 | Statistical analysis

Unpaired *t*-tests were used to compare two groups of samples. Additionally, one-way analysis of variance was employed for comparison among three or more groups. Dunnett's test was also applied to determine differences between multiple groups, with *p* < 0.05 being considered statistically significant.

### 3 | RESULTS

#### 3.1 | PROM1 is expressed in the seminiferous tubules of the testis and is essential for germ cell maintenance

First, we attempted to verify the correlation between genotyping PCR and actual protein expression. To this end, genomic PCR was

performed in *Prom1*-mutant mice (Figure S1A,B), with PROM1 protein expression being confirmed through western blotting of samples that provided different PCR band sizes (Figure S1B). The western blotting was performed using tissue samples extracted from the kidney and testes since these have been shown to have a high PROM1 expression. The results subsequently confirmed a complete loss of PROM1 expression in samples that provided 600bp PCR fragments, while clear bands were observed at the expected size from samples

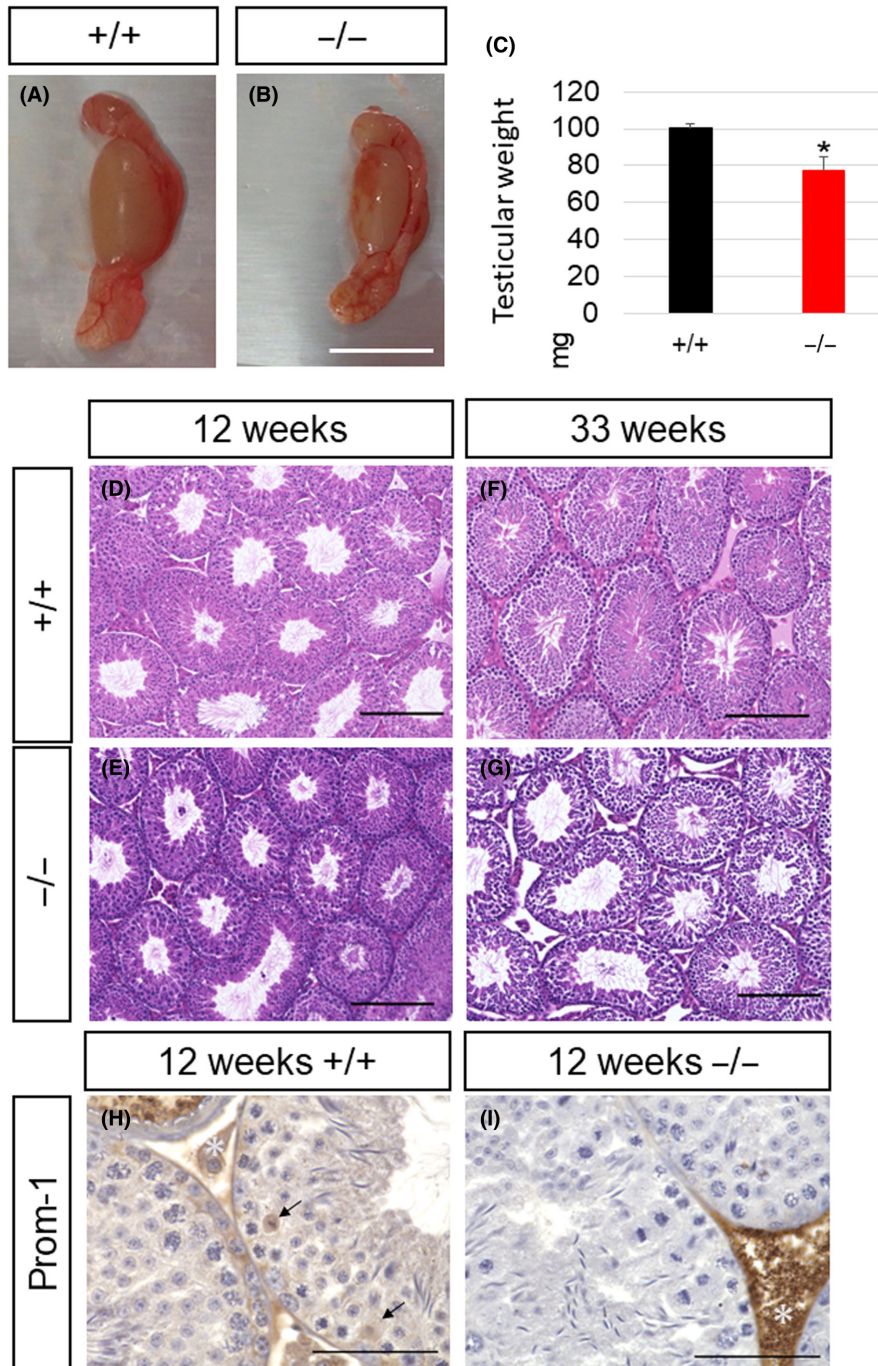


**FIGURE 1** Gross appearance and histology of the testis. (A, B) Gross appearance of testis from 12-week-old *Prom1*<sup>+/+</sup> (A) and *Prom1*<sup>-/-</sup> (B) mice. Scale bar = 5 mm. (C) Quantification of testicular volume in WT and *Prom1* KO mice. Error bars indicate standard error (SEM), Student's *t*-test, *n* = 5, \**p* < 0.05. (D–G) Hematoxylin and eosin staining of testis cross-sections from 12- and 33-week-old mice. Scale bar = 200 μm. (H, I) Immunohistostaining of PROM1. Specific and non-specific signals are indicated using arrows and asterisks, respectively. Scale bar = 50 μm.



that provided 240bp PCR fragments (Figure S1B–D). Therefore, genotyping PCR and actual expression corresponded well. Next, to analyze the effect of *Prom1* gene deficiency on reproductive organs, we analyzed overall appearance of the testis and epididymis. The testes with epididymis were extracted from 12-week-old male *Prom1*<sup>-/-</sup> and wild-type (*Prom1*<sup>+/+</sup>) mice and the appearance was observed. As a result, the testes size of *Prom1* KO mice was smaller than that of WT mice (Figure 1A,B). Consistently, the weight of the testes was lower in *Prom1*<sup>-/-</sup> mice (78 ± 6.9 mg, *n* = 5) compared to those in the *Prom1*<sup>+/+</sup> mice (101 ± 1.6 mg, *n* = 5; *p* < 0.05) (Figure 1C). These observations suggest that testis growth was, at least in part, perturbed by the attenuation of the PROM1 function.

Next, we investigated the structure of the seminiferous tubules of testes of 12- and 33-week-old *Prom1*<sup>-/-</sup> mice. While no apparent differences were observed at 12 weeks in the seminiferous tubules of *Prom1*<sup>+/+</sup> and *Prom1*<sup>-/-</sup> testes (Figure 1D,E), a drastic loss of germ cells in the seminiferous tubules was noted in the *Prom1*<sup>-/-</sup> mice compared to those in the *Prom1*<sup>+/+</sup> mice at 33 weeks (Figure 1F,G). Moreover, PROM1 was localized in the cytoplasm of some mitotic spermatocytes at 12 weeks in the *Prom1*<sup>+/+</sup> testis (brown signal in Figure 1H); however, no such signals were

detected in the corresponding area in the *Prom1*<sup>-/-</sup> specimen (Figure 1I).

Next, we attempted to identify the cells that express *Prom1* in the testis and epididymis and took advantage of the *LacZ* gene that had been knocked in at the *Prom1* locus in *Prom1*-mutant mice.

At 3 weeks of age, when the male mice were not yet sexually mature, there was no staining for β-gal in the testis of both WT (negative control) and heterozygous mutants (*Prom1*<sup>+/-</sup>), suggesting that PROM1 protein is not expressed, or if any, at very low levels (Figure 2A,B). In contrast, in the testes of 8-week-old mice, the age at which mice are sexually mature, strong β-gal staining was noted in the inner part of the seminiferous tubules of *Prom1* heterozygous mutants (Figure 2C,D).

The positive cells positive for β-gal staining were observed in the epididymal tubules of the heterozygous mutants (Figure S2A,B). Thus, *Prom1* is already expressed in the epididymis at 3 weeks in mice. Also, the evident signal was found in columnar epithelial cells of the epididymis at 8 weeks of age (Figure S2C,D).

Altogether, these findings suggest that PROM1 is expressed in the differentiating germ cells and epididymal epithelial cells and is involved in the proliferation and maturation of the spermatozoa.

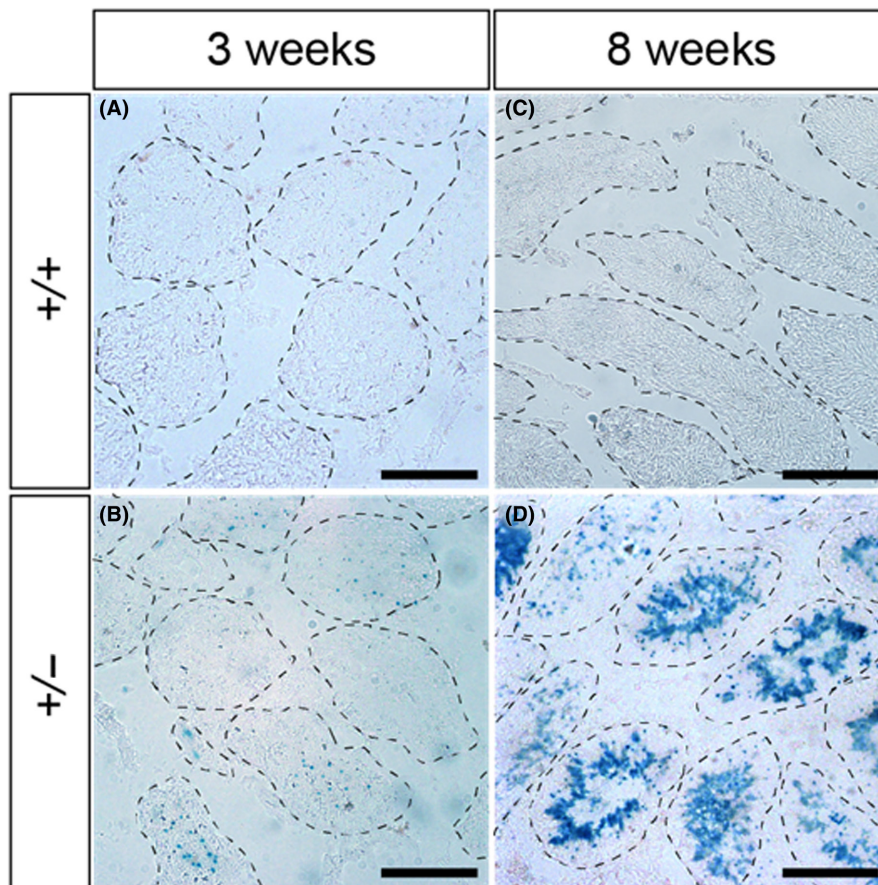


FIGURE 2 PROM1 is expressed at the seminiferous tubules in the testis. Three- (A, C) and eight- (B, D) week-old *Prom1*<sup>+/+</sup> (A, B), and *Prom1*<sup>+/-</sup> (C, D) male mice were subjected to β-gal staining assay. Scale bars = 50 μm.

### 3.2 | *Prom1*-mutant male, but not female, mice are infertile

We next sought to evaluate the effect of *Prom1* deficiency on breeding potential.

For this, we arranged breeding pairs of different genotypes consisting of male mice aged 8 weeks and heterologous females of the same age, with the total number of offspring being counted every month. As a result, while the *Prom1*<sup>+/+</sup> male mice maintained fertility until the end of the examination, heterozygous mice showed a decreasing breeding potential over time, suggesting that *Prom1* heterozygote had a partially infertile phenotype that became more severe with age (Figure 3A). The total number of pups born by the time the mouse reached 6 months of age was an average of  $76.7 \pm 13.8$  in *Prom1*<sup>+/+</sup> males. By contrast, heterozygous male mice produced significantly smaller litters of  $17.7 \pm 3.2$  pups ( $p < 0.05$ ), suggesting that the *Prom1* gene expressed an incompletely dominant trait with respect to the breeding potential. However, mating with *Prom1*<sup>-/-</sup> male mice did not produce any pups ( $p < 0.05$ ) (Figure 3B).

We next investigated whether the female genotype had an effect on the infertility phenotype. We, thus, assessed the breeding potential of female WT and *Prom1* mutants, both at 8 weeks of age. In WT mice, pups were born an average of 28 days after the start of mating. When *Prom1*<sup>+/+</sup> and *Prom1*<sup>-/-</sup> female mice were crossed

with *Prom1* heterozygous male mice, pups were also born within 28–30 days. Therefore, the genotype of female mice did not affect fertility. However, crosses between male *Prom1*<sup>-/-</sup> mice and WT female mice did not yield any pups (Figure 3C).

Overall, this examination suggested that the infertility phenotype resulting from the *Prom1* mutation was solely caused by the loss of male reproductive function.

### 3.3 | PROM1 plays an essential role in inhibiting apoptosis

The decreased cell density in the seminiferous tubules of *Prom1* KO mice (Figure 1) prompted us to examine the possibility of programmed cell death in the testes of the *Prom1*-mutant mice. Because apoptosis may have already occurred at less than 12 weeks of age, we extracted the testes from 4-, 8-, and 12-week-old WT and *Prom1* KO mice and performed TUNEL staining. We observed that the number of TUNEL-positive cells in the seminiferous tubules of *Prom1*<sup>-/-</sup> and *Prom1*<sup>+/-</sup> mice were significantly higher than that in the WT mice (Figure 4A), indicating that PROM1 has a protective role against germ cell apoptosis. Furthermore, most TUNEL-positive germ cells were mitotic spermatocytes (Figure 4B,C). When the number of apoptotic cells was counted only in stage 12 seminiferous tubules where the spermatocyte division occurred, the apoptosis index was found to

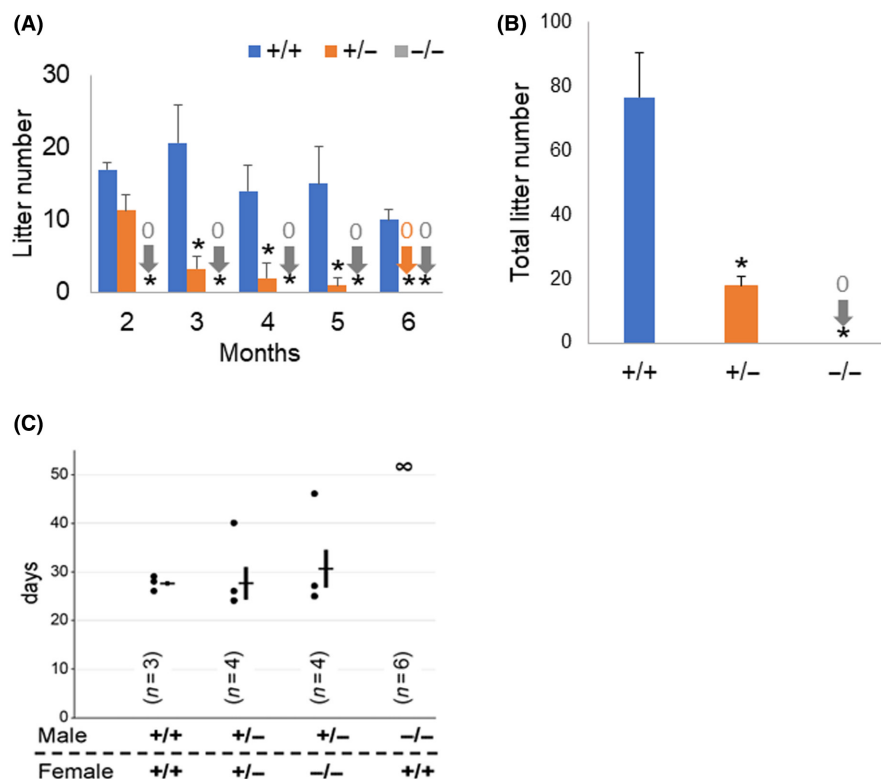


**FIGURE 3** *Prom1* male mice exhibit the infertile phenotype. (A) Breeding potential of *Prom1*-mutant mice and number of litters per month. (B) Total litter number produced by the breeding pairs of *Prom1*<sup>-/-</sup> and *Prom1*<sup>+/+</sup> mice over a 6-month period. Statistical significances were analyzed between the WT and each genotype. Error bars indicate SEM,  $n = 3$ , Dunnett's test,  $*p < 0.05$ . (C) Number of days until birth for various breeding pairs.

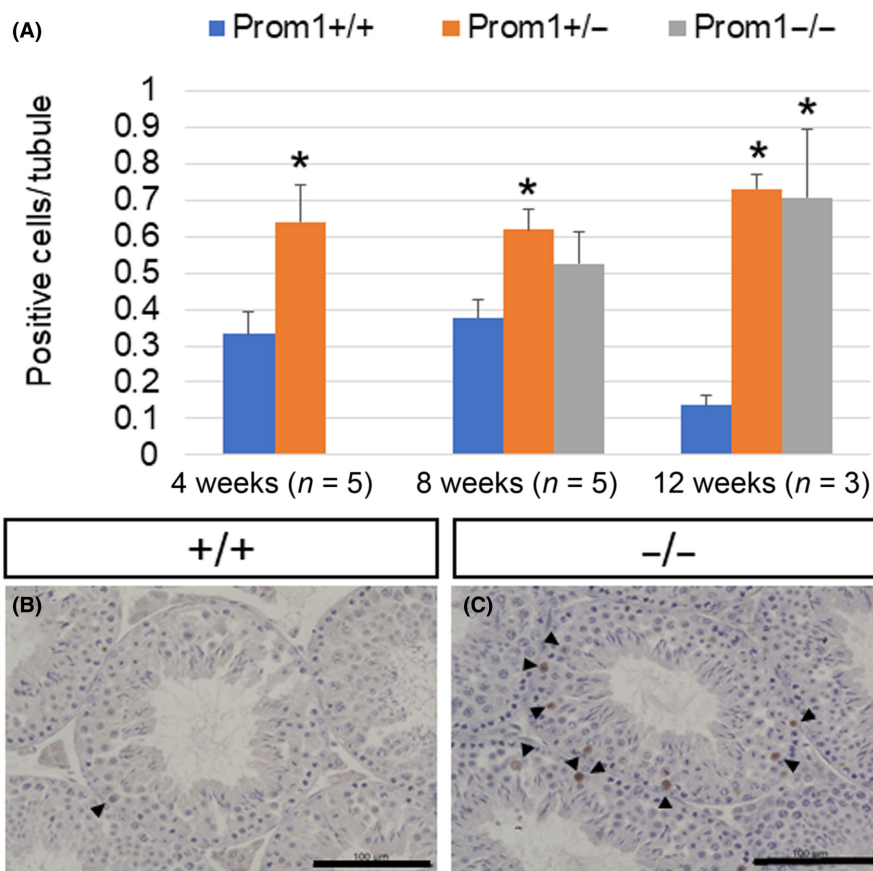


**FIGURE 4** Anti-apoptotic effect of PROM1. (A) Percentage of apoptotic cells (TUNEL-positive cells/semiferous tubules). Error bars indicate SEM, Dunnett's test,  $*p < 0.05$ . w, weeks. (B, C) TUNEL staining of seminiferous tubules from 12-week-old mice. Scale bar = 100  $\mu\text{m}$ . Black arrows indicate TUNEL-positive cells.

have been significantly increased in *Prom1*<sup>-/-</sup> mice compared to that in WT mice both at 8 and 12 weeks of ages (Figure 3A,B). Overall, these findings suggest that PROM1 functions during cell division, and its deficiency, cause cell death in the dividing cells.

### 3.4 | PROM1 is essential for maintenance of proliferation of sperm epithelial cells

To further investigate the function of PROM1 in inhibiting programmed cell death, we analyzed the frequency of phosphorylated histone H3 (pHH3)-positive mitotic phase cells using immunofluorescence on the testis from 12-week-old *c* and *Prom1*<sup>-/-</sup> mice. As a result, we observed a drastic decrease in the number of pHH3-positive cells in the seminiferous tubules of *Prom1*<sup>-/-</sup> mice (Figure 5A–D).<sup>30</sup> Furthermore, western blotting analysis revealed a significant decrease in the accumulation of the pHH3 protein in the *Prom1*<sup>-/-</sup> mice (32.4%,  $p < 0.05$ ) compared to that in the *Prom1*<sup>+/+</sup> mice (Figure 5E,F).

We further sought the underlying mechanisms and speculated that PROM1 protects against programmed cell death via c-FLIP because c-FLIP is a major apoptosis suppressor protein in sperm epithelial cells.<sup>31–33</sup> As expected, western blotting analysis demonstrated

that c-FLIP expression was significantly decreased in testis of *Prom1*<sup>-/-</sup> mice (56.6%,  $p < 0.05$ ) (Figure 5E,G). We further examined the expression of phosphorylated ERK1/2 (pERK1/2) because the activation of ERK1/2 coincides with cell proliferation and plays an important role in spermatogenesis. The western blot analysis revealed that the pERK1/2 expression was significantly decreased in *Prom1*<sup>-/-</sup> mice testes (54.8%,  $p < 0.05$ ) (Figure 5E,H).

Taken together, these findings suggest that PROM1 is essential for the promotion of cell division and suppression of programmed cell death via the maintenance of c-FLIP and activation of ERK.

### 3.5 | PROM1 deficiency causes abnormal morphology of sperm flagella

Finally, we investigated the effect of *Prom1* deficiency on sperm morphology. First, we assessed the epididymal sperm quality of 8-week-old *Prom1*<sup>-/-</sup> mice, and a significantly higher number of spermatozoa was found with abnormal morphologies, shorter and angled (Figure 6A–D, Figure S4). The malformation rate in *Prom1* KO mice was significantly higher than that in the WT mice (8 weeks:  $63 \pm 6.5\%$  vs.  $32.8 \pm 3.5\%$ ,  $p < 0.05$  and 12 weeks:  $93.2 \pm 3.6\%$  vs.  $28 \pm 5.4\%$ ,  $p < 0.05$ ) (Figure 6C,D).

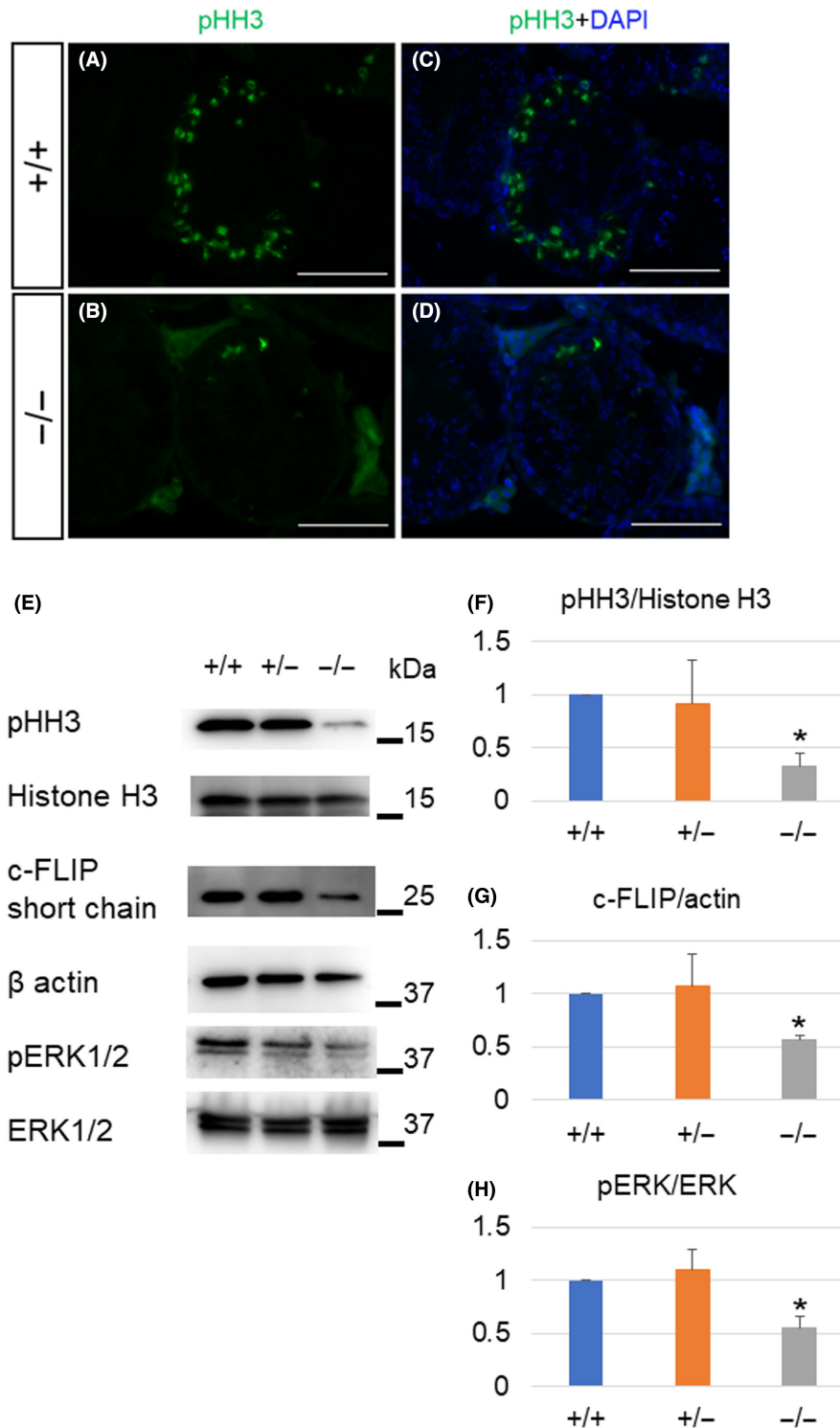


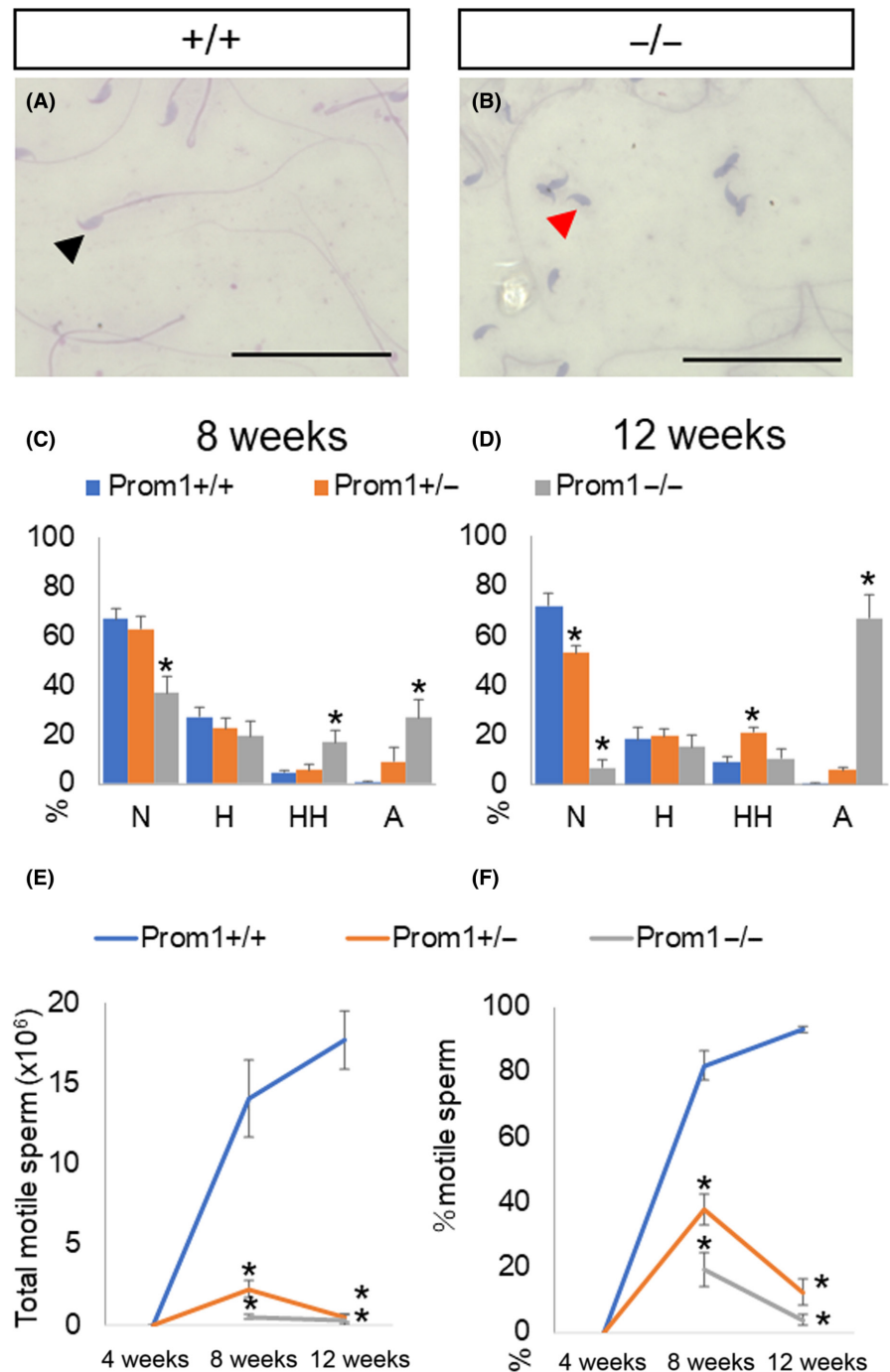
**FIGURE 5** Proliferation analysis of the *Prom1*<sup>-/-</sup> mice. (A–D) Immunofluorescence analysis of seminiferous tubules. The nucleus was stained with DAPI (blue), and pHH3 was targeted using a monoclonal antibody (green). (E–H) Western blotting analysis of pHH3, c-FLIP, and pERK1/2 of mouse testes. (E) Expression of each protein was measured via western blotting analysis of protein lysates obtained from mouse testes. (F–H) Quantification of each protein expression with respect to actin expression. Actin, histone H3, and ERK1/2 were set as the loading controls, and data of wild types were arbitrarily set as 1.  $N=4$ , error bars indicate SEM. Dunnett's test, \* $p < 0.05$ .

We further assessed the motility of spermatozoa of 4-, 8-, and 12-week-old WT and *Prom1*<sup>-/-</sup> mice. In the WT mice, the number of motile sperm in the epididymis increased as the mice got matured,

and more than 80% of the spermatozoa were motile at 8 and 12 weeks. In contrast, in the *Prom1*<sup>+/-</sup> and *Prom1*<sup>-/-</sup> mice, the number of motile spermatozoa was significantly lower than that in WT



**FIGURE 6** Morphology of epididymal spermatozoa. (A, B) Appearance of spermatozoa in each genotype. Black arrows and red arrows indicate normal spermatozoa and no-tail spermatozoa, respectively. (C, D) Comparisons of sperm abnormality. A, Absent; H, Hairpin; HH, Half-hairpin; N, Normal spermatozoa. (E, F) Total motile sperm percentage of motile sperm upon release and incubation in vitro. Error bars indicate SEM,  $n=5$ , Dunnett's test,  $*p<0.05$ .



mice (Figure 6E,F), and motile spermatozoa were hardly detected at 12 weeks.

Taken together, these findings suggest that *Prom1* deficiency causes abnormal morphology and impairs the motility of spermatozoa.

## 4 | DISCUSSION

Understanding the pathogenic mechanisms underlying spermatogenic disorders is crucial for diagnosing and establishing novel treatments for male infertility, particularly NOA. A recent study revealed the relationship between PROM1 and NOA and described the

involvement of PROM1 in spermatogenic impairment.<sup>27</sup> The present study provides direct evidence that PROM1 plays multiple roles in cell proliferation and survival in seminiferous tubules and sperm morphology and motility in mice.

*Prom1* KO mice in our study exhibited reduced testicular weight and seminiferous tubule thickness at 33 weeks (Figure 1A-C,F,G), indicating that PROM1 plays an important role in spermatogenesis. Our immunohistochemistry results suggest that PROM1 is highly expressed in the diakinesis phase in spermatocytes (Figure 1H,I). Moreover, PROM1 was localized in the spermatozoa and columnar epithelium of the epididymis (Figure 2E-H). Although the above results were from  $\beta$ -gal staining and did not completely reflect the

actual localization, the observations are in agreement with those of physiological studies that reported that PROM1 is expressed in sperm flagella.<sup>25,27</sup> Furthermore, our fertility tests revealed that the functional deletion of *Prom1* resulted in complete infertility (Figure 3). Overall, PROM1 protects cell survival during cell division in sperm epithelial cells and influences the morphology of sperm flagella. Its deficiency inhibits cell division, enhances programmed cell death, and impairs motility of spermatozoa, thereby resulting in male infertility.

It is well known that the balance between cell proliferation and apoptosis is essential in spermatogenesis and that instability in this balance causes infertility.<sup>34,35</sup> Additionally, spermatogonia and spermatocytes are vulnerable to apoptotic signals and, thus, are the main sites of apoptosis during spermatogenesis.<sup>36</sup> Our TUNEL assay results revealed that apoptotic signals appeared mainly in dividing spermatocytes in the *Prom1*<sup>-/-</sup> mice (Figure 4A–C). In addition, the expression of pHH3, a mitotic phase marker, was significantly decreased in the *Prom1*<sup>-/-</sup> mice, suggesting that PROM1 is also involved in spermatogenic cell division (Figure 5A–F). These results, therefore, indicate that PROM1 plays an important role in regulating germ cell number through apoptosis and cell division.

Previous studies have investigated the role of PROM1 in patients with NOA<sup>27</sup> and reported that PROM1 is involved in spermatogenesis as well as in sperm flagella morphology. Our present study suggests that PROM1 promotes c-FLIP expression (Figure 5E,G) and ERK activation (Figure 5E,H). Furthermore, it has been shown that c-FLIP blocks the pathway that converts procaspase 8 to caspase 8, and thereby suppresses apoptosis via FAS signaling in cancer stem cells.<sup>18</sup> It has also been reported that c-FLIP is expressed in germ cells and protects them from FAS-dependent apoptosis.<sup>31,33</sup> In addition, c-FLIP is predominantly expressed in spermatocytes and spermatids, whereas its expression is lower in spermatogonia.<sup>33</sup>

In parallel with the c-FLIP activity, a previous study revealed that ERK is expressed throughout spermatogenesis, and ERK phosphorylation is essential in spermatocyte division.<sup>37</sup> Previous studies have also shown that in cancer cells, PROM1 promotes c-FLIP expression, and its activation results in the expression of downstream signaling factors involved in cell division and cell survival, including ERK, Akt, Wnt, and c-Jun.<sup>20–23</sup> Taking into consideration the findings of the previous studies and the present study, it is reasonable to assume that c-FLIP is a factor that activates ERK, which in turn is involved in germ cell division. Further investigations are necessary to elucidate the mechanisms of cell division and apoptosis.

PROM1 expression has been reported in various epithelial cells,<sup>4,38–41</sup> with several different splice variants being expressed in different organs, and some specific isoforms, are predominantly expressed in the testis and epididymis.<sup>25</sup> Plasma membrane protrusions are regulated by *Prom1*.<sup>27,38</sup> Therefore, these variants are thought to be involved in the morphological maintenance of stereocilia in the epididymis and flagella in the sperm.<sup>25</sup> Another report showed that PROM1 is localized in sperm flagella and plays

an important role in spermiogenesis.<sup>27</sup> Furthermore, *Prom1*<sup>-/-</sup> mice showed an increased percentage of abnormal sperm flagella and decreased motility (Figure 6C–F), corroborating the previously reported role of PROM1.<sup>25,27,41</sup> It remains unclear whether the mechanisms that caused morphological abnormalities were based on the same as those that ensured cell survival. However, it is easily conceivable that spermatozoa produced through abnormal cell division would have abnormal morphology. Moreover, PROM1 is a cholesterol-binding protein<sup>42</sup> and may play a role in the formation and morphological maintenance of the flagellum. In addition, it was found that PROM1 was expressed in the epididymis (Figure S2); therefore, the maturation process of spermatozoa may have been affected by the dysfunction of epididymis in *Prom1*<sup>-/-</sup> mice. In this regard, anti-estrogen therapy and estrogen receptor KO reportedly suppresses sperm maturation, and the former causes a decrease in *Prom1* expression in the *caput epididymis*, which may suppress sperm maturation.<sup>41</sup> The reduced number of motile sperm in the *Prom1*<sup>-/-</sup> mice and the accumulation of PROM1 in stereocilia suggest that PROM1 in the columnar epithelial cells of the epididymis affects sperm motility. Further investigations are required to clarify the role of PROM1 in sperm morphology and motility.

Our study has several limitations. First, although this study is focused on c-FLIP and ERK activation, a comprehensive analysis of the pathways through which c-FLIP affects ERK, as well as other signaling pathways associated with c-FLIP, is required. Second, as this is an in vivo observational study, the mechanisms in which PROM1 is involved in sperm flagellum formation remains unclear.

In summary, our results collectively indicate that PROM1 plays a prominent role in spermatogenesis. During spermatogenesis, PROM1 presumably promotes c-FLIP transcription and ERK activation. Accumulating further evidence regarding the regulation of *Prom1* expression may open avenues to improve spermatogenesis and sperm quality using PROM1-based molecular approaches.

## ACKNOWLEDGMENTS

This project was supported by a Grant-in-Aid for Scientific Research (C) (22K09475) from the Japan Society for the Promotion of Science. We would also like to thank Editage ([www.editage.com](http://www.editage.com)) for English language editing.

## CONFLICT OF INTEREST STATEMENT

The authors declare no conflict of interest.

## ETHICS STATEMENT

All animal experiments were approved by the Committees for Ethics on Animal Experiments of Yamaguchi University School of Medicine (J16021) and Nara Institute of Science and Technology.

## ANIMAL STUDIES

All institutional and national guidelines for the care and use of laboratory animals were followed.

## ORCID

Haruka Matsukuma  <https://orcid.org/0000-0001-5634-6957>

Koji Shiraiishi  <https://orcid.org/0000-0002-3278-7747>

## REFERENCES

- Oakberg EF. Duration of spermatogenesis in the mouse and timing of stages of the cycle of the seminiferous epithelium. *Am J Anat.* 1956;99(3):507–16.
- Miraglia S, Godfrey W, Yin AH, Atkins K, Warnke R, Holden JT, et al. A novel five-transmembrane hematopoietic stem cell antigen: isolation, characterization, and molecular cloning. *Blood.* 1997;90(12):5013–21.
- Yin AH, Miraglia S, Zanjani ED, Almeida-Porada G, Ogawa M, Leary AG, et al. AC133, a novel marker for human hematopoietic stem and progenitor cells. *Blood.* 1997;90(12):5002–12.
- Weigmann A, Corbeil D, Hellwig A, Huttner WB. Prominin, a novel microvilli specific polytopic membrane protein of the apical surface of epithelial cells, is targeted to plasma membrane protrusions of non epithelial cells. *Proc Natl Acad Sci USA.* 1997;94:12425–30.
- Hori A, Nishide K, Yasukuni Y, Haga K, Kakuta W, Ishikawa Y, et al. Prominin-1 modulates rho/ROCK-mediated membrane morphology and calcium-dependent intracellular chloride flux. *Sci Rep.* 2019;9(1):15911.
- Jang JW, Song Y, Kim SH, Kim J, Seo HR. Potential mechanisms of CD133 in cancer stem cells. *Life Sci.* 2017;184:25–9.
- Zhao P, Lu Y, Jiang X, Li X. Clinicopathological significance and prognostic value of CD133 expression in triple-negative breast carcinoma. *Cancer Sci.* 2011;102(5):1107–11.
- Brescia P, Ortensi B, Fornasari L, Levi D, Broggi G, Pelicci G. CD133 is essential for glioblastoma stem cell maintenance. *Stem Cells.* 2013;31(5):857–69.
- Mardani A, Gheytaichi E, Mousavie SH, Madjd Jabari Z, Shooshtarizadeh T. Clinical significance of cancer stem cell markers CD133 and CXCR4 in osteosarcomas. *Asian Pac J Cancer Prev.* 2020;21(1):67–73.
- Korn P, Kampmann A, Spalthoff S, Jehn P, Tavassol F, Lentge F, et al. Suitability of CD133 as a marker for cancer stem cells in melanoma. *Asian Pac J Cancer Prev.* 2021;22(5):1591–7.
- Hilbe W, Dirnhofer S, Oberwasserlechner F, Schmid T, Gunsilius E, Hilbe G, et al. CD133 positive endothelial progenitor cells contribute to the tumour vasculature in non-small cell lung cancer. *J Clin Pathol.* 2004;57(9):965–9.
- Ma S. Biology and clinical implications of CD133<sup>+</sup> liver cancer stem cells. *Exp Cell Res.* 2013;319(2):126–32.
- Kojima M, Ishii G, Atsumi N, Fujii S, Saito N, Ochiai A. Immunohistochemical detection of CD133 expression in colorectal cancer: a clinicopathological study. *Cancer Sci.* 2008;99(8):1578–83.
- Immervoll H, Hoem D, Sakariassen PO, Steffensen OJ, Molven A. Expression of the "stem cell marker" CD133 in pancreas and pancreatic ductal adenocarcinomas. *BMC Cancer.* 2008;8:48.
- Kim K, Ro JY, Kim S, Cho YM. Expression of stem-cell markers OCT-4 and CD133: important prognostic factors in papillary renal cell carcinoma. *Hum Pathol.* 2012;43(12):2109–16.
- Farid RM, Sammour SA, Shehab EIDin ZA, Salman MI, Omran TI. Expression of CD133 and CD24 and their different phenotypes in urinary bladder carcinoma. *Cancer Manag Res.* 2019;11:4677–90.
- Yang Y, Liu Z, Wang Q, Chang K, Zhang J, Ye D, et al. Presence of CD133-positive circulating tumor cells predicts worse progression-free survival in patients with metastatic castration-sensitive prostate cancer. *Int J Urol.* 2022;29(5):383–9.
- Barzegar Behrooz A, Syahir A, Ahmad S. CD133: beyond a cancer stem cell biomarker. *J Drug Target.* 2019;27(3):257–69.
- Zobalova R, McDermott L, Stantic M, Prokopova K, Dong LF, Neuzil J. CD133-positive cells are resistant to TRAIL due to up-regulation of FLIP. *Biochem Biophys Res Commun.* 2008;373(4):567–71.
- Kim MJ, Kim HB, Bae JH, Lee JW, Park SJ, Kim DW, et al. Sensitization of human K562 leukemic cells to TRAIL-induced apoptosis by inhibiting the DNA-PKcs/Akt-mediated cell survival pathway. *Biochem Pharmacol.* 2009;78(6):573–82.
- Kataoka T, Tschopp J. N-terminal fragment of c-FLIP(L) processed by caspase 8 specifically interacts with TRAF2 and induces activation of the NF-kappaB signaling pathway. *Mol Cell Biol.* 2004;24(7):2627–36.
- Nakajima A, Komazawa-Sakon S, Takekawa M, Sasazuki T, Yeh WC, Yagita H, et al. An antiapoptotic protein, c-FLIPL, directly binds to MKK7 and inhibits the JNK pathway. *EMBO J.* 2006;25(23):5549–59.
- Naito M, Katayama R, Ishioka T, Suga A, Takubo K, Nanjo M, et al. Cellular FLIP inhibits beta-catenin ubiquitylation and enhances Wnt signaling. *Mol Cell Biol.* 2004;24(19):8418–27.
- Lavrik IN, Krammer PH. Regulation of CD95/Fas signaling at the DISC. *Cell Death Differ.* 2012;19(1):36–41.
- Fargeas CA, Joester A, Missol-Kolka E, Hellwig A, Huttner WB, Corbeil D. Identification of novel Prominin-1/CD133 splice variants with alternative C-termini and their expression in epididymis and testis. *J Cell Sci.* 2004;117(Pt 18):4301–11.
- Kemper K, Tol MJ, Medema JP. Mouse tissues express multiple splice variants of prominin-1. *PLoS One.* 2010;5(8):e12325.
- Yukselten Y, Aydos OSE, Sunguroglu A, Aydos K. Investigation of CD133 and CD24 as candidate azoospermia markers and their relationship with spermatogenesis defects. *Gene.* 2019;706:211–21.
- Dellett M, Sasai N, Nishide K, Becker S, Papadaki V, Limb GA, et al. Genetic background and light-dependent progression of photoreceptor cell degeneration in Prominin-1 knockout mice. *Invest Ophthalmol Vis Sci.* 2014;56(1):164–76.
- Nishide K, Nakatani Y, Kiyonari H, Kondo T. Glioblastoma formation from cell population depleted of Prominin1-expressing cells. *PLoS One.* 2009;4(8):e6869.
- Song N, Liu J, An S, Nishino T, Hishikawa Y, Koji T. Immunohistochemical analysis of histone H3 modifications in germ cells during mouse spermatogenesis. *Acta Histochem Cytochem.* 2011;44(4):183–90.
- Chandrasekaran Y, McKee CM, Ye Y, Richburg JH. Influence of TRP53 status on FAS membrane localization, CFLAR (c-FLIP) ubiquitylation, and sensitivity of GC-2spd (ts) cells to undergo FAS-mediated apoptosis. *Biol Reprod.* 2006;74(3):560–8.
- Giampietri C, Petrunaro S, Coluccia P, D'Alessio A, Starace D, Riccioli A, et al. Germ cell apoptosis control during spermatogenesis. *Contraception.* 2005;72(4):298–302.
- Giampietri C, Petrunaro S, Coluccia P, D'Alessio A, Starace D, Riccioli A, et al. FLIP is expressed in mouse testis and protects germ cells from apoptosis. *Cell Death Differ.* 2003;10(2):175–84.
- Kimura M, Itoh N, Takagi S, Sasao T, Takahashi A, Masumori N, et al. Balance of apoptosis and proliferation of germ cells related to spermatogenesis in aged men. *J Androl.* 2003;24(2):185–91.
- Takagi S, Itoh N, Kimura M, Sasao T, Tsukamoto T. Spermatogonial proliferation and apoptosis in hypospermatogenesis associated with nonobstructive azoospermia. *Fertil Steril.* 2001;76(5):901–7.
- Dadhich RK, Real FM, Zurita F, Barrionuevo FJ, Burgos M, Jimenez R. Role of apoptosis and cell proliferation in the testicular dynamics of seasonal breeding mammals: a study in the Iberian mole, *Talpa occidentalis*. *Biol Reprod.* 2010;83(1):83–91.
- Inselman A, Handel MA. Mitogen-activated protein kinase dynamics during the meiotic G2/MI transition of mouse spermatocytes. *Biol Reprod.* 2004;71(2):570–8.

38. Corbeil D, Roper K, Hellwig A, Tavian M, Miraglia S, Watt SM, et al. The human AC133 hematopoietic stem cell antigen is also expressed in epithelial cells and targeted to plasma membrane protrusions. *J Biol Chem*. 2000;275(8):5512–20.
39. Karbanova J, Corbeil D, Fargeas CA. Prominin-1/CD133, saliva and salivary glands—integrating existing data to new clinical approaches. *Exp Cell Res*. 2019;383(2):111566.
40. Bhattacharya S, Yin J, Winborn CS, Zhang Q, Yue J, Chaum E. Prominin-1 is a novel regulator of autophagy in the human retinal pigment epithelium. *Invest Ophthalmol Vis Sci*. 2017;58(4):2366–87.
41. Pereira MF, Fernandes SA, Nascimento AR, Siu ER, Hess RA, Oliveira CA, et al. Effects of the oestrogen receptor antagonist Fulvestrant on expression of genes that affect organization of the epididymal epithelium. *Andrology*. 2014;2(4):559–71.
42. Corbeil D, Marzesco AM, Fargeas CA, Huttner WB. Prominin-1: a distinct cholesterol-binding membrane protein and the organisation of the apical plasma membrane of epithelial cells. *Subcell Biochem*. 2010;51:399–423.

## SUPPORTING INFORMATION

Additional supporting information can be found online in the Supporting Information section at the end of this article.

**How to cite this article:** Matsukuma H, Kobayashi Y, Oka S, Higashijima F, Kimura K, Yoshihara E, et al. *Prominin-1* deletion results in spermatogenic impairment, sperm morphological defects, and infertility in mice. *Reprod Med Biol*. 2023;22:e12514. <https://doi.org/10.1002/rmb2.12514>